19th Australasian Fluid Mechanics Conference
Melbourne, Australia
8-11 December 2014

Validation of a Microbubble Seeding Generator for Particle Image Velocimetry Applications

G. A. Zarruk[1], A. D. Henderson[1], K. L. de Graaf[1], and P. A. Brandner[1], and B. W. Pearce[1]

[1]Australian Maritime College
University of Tasmania, Launceston 7250, TAS, Australia

[2]School of Engineering and ICT
University of Tasmania, Hobart 7001, TAS, Australia

Abstract

Particle Image Velocimetry, using solid particles or oil droplets as tracers, is an effective technique to characterize a wide variety of flow phenomena. Unfortunately, there are cases in which the use of these type of tracers is not an option, such as cavitating flows where the presence of particles will influence the occurrence of cavitation, or multi-phase flows where the interfacial behavior may be modified. In these, the use of microbubbles as tracers is an option. Microbubbles can be generated with nozzles designed to trigger a rapid expansion of supersaturated liquid. A prototype microbubble generator was designed and manufactured to be used as a seeding generator for PIV applications. The viability of the microbubble generator and microbubbles as seeding was tested using a two-dimensional turbulent planar jet; a flow comprehensively described in the existing literature. Time-Resolved PIV experiments were carried at a jet exit Reynolds numbers of $Re = 10,000$. The mean and turbulent velocity fields, and coherent structures resolved by proper orthogonal decomposition, from the jet exit to about 20 jet heights, are presented and compared against previously published results. The results show that the use of microbubbles as a flow tracer is suitable for PIV applications in turbulent flows. Further work is required to characterize the microbubble generator and establish the uncertainty of the results relative to the use of particles as seeding.

Introduction

Particle Image Velocimetry (PIV) has been a popular experimental technique for the past decades. The technique has developed rapidly and has been used to study a wide variety of flows and phenomena. However, there remain cases in which PIV can not be used due to the type of tracer used to resolve the flow. In most cases, solid particles are used for liquid flows and oil droplets for gas flows. Unfortunately, these type of tracers are not an option in multiphase flows where the presence of particles might influence the interfacial behavior (eg., air-liquid interface). Furthermore, introducing particles or droplets in some research facilities is not possible or undesirable. The latter is what motivates the present work. Using particles in a water tunnel designed for cavitation studies is not possible. The presence of particles will influence the occurrence of cavitation, and completely removing particles from the experimental facilities would be an almost impossible and costly task.

An alternative to particles is the use of bubbles as seeding. Using bubbles to trace the movement of the fluids is not a new concept. As bubbles occur naturally in many flows, they can be used to resolve the velocity field using a Bubble Image Velocimetry (BIV) algorithm [13]. This method relies on the natural presence of bubbles of different sizes and correlating the texture of the bubble images. For flows without bubbles it is necessary to seed the flow with microbubbles and use traditional PIV algorithms to resolve the velocity field.

There are several methods to produce microbubbles suitable for PIV applications. Recently lab-on-chip devices have been developed for production of mono-dispersed populations for a range of application, including contrast agents for medical diagnostics [9]. Microbubble production rates from these devices are however too low for many PIV applications. the most practical method, although producing polydispersed populations, is throug the rapid expansion of super-saturated water through a micro-passage [12]. The same concept can be used in a miniature confined miniature turbulent round jet [2], or with rotating porous circular plates [6]. Another method is the use of electrolysis and a venturi to generate and control the size of the microbubbles [20].

The studies above on microbubble generation focus on the method, bubble size distribution, and production rate. However, microbubbles are rarely used in PIV experiments. Although it is expected that microbubbles will follow the flow due to their small relaxation time, there are several other parameters that could affect the viability of microbubbles as PIV tracers, such as the light scattering properties of the bubbles and the bubble image size.

In this paper we present a method to generate microbubbles as seeding for PIV applications. The generator and microbubbles as tracer are validated in an experiment using a turbulent two-dimensional planar jet. The results presented here describe the mean and turbulent velocity fields of the jet and compare them with previously publish works. The coherent structures of the jet, resolved using proper orthogonal decomposition of the flow field, are also presented.

Experimental Setup and Methods

An schematic representation of the experimental setup and microbubble generator are presented in Figure 1. The nozzle is a confined radial jet of 8 mm outer diameter and 1 mm inner diameter, respectively, and height of 0.01 mm [1]. The supersaturated water for microbubble generation is supplied from a saturation vessel that was pressurized to 1 MPa. The saturation vessel consists of an ancillary circuit to aid rapid saturation. The vessel water is recirculated through a venturi with a perforated throat to ingest air and enhance the dissolution process. The saturation vessel pressure is measured using a WIKA Model P-30 absolute pressure transducer with a precision of 0.1%. Atmospheric pressure is measured using a Vaisala Model PTB 210 digital barometer with a precision of ± 0.03 kPa. The dynamic dissolved O_2 concentration and temperature during initial saturation are measured using a Hach Ultra Orbisphere Model A1100 EC dissolved O_2 sensor. The flow rate of the injected supersaturated water is measured using the time rate of change of a level sensor, recorded using a National Instruments 6341 data acquisition card. The level sensor is an Orion Instruments magnetically coupled liquid level sensor. The estimated precision of the microbubble generator flow rate measurement is $< \pm 0.5\%$.

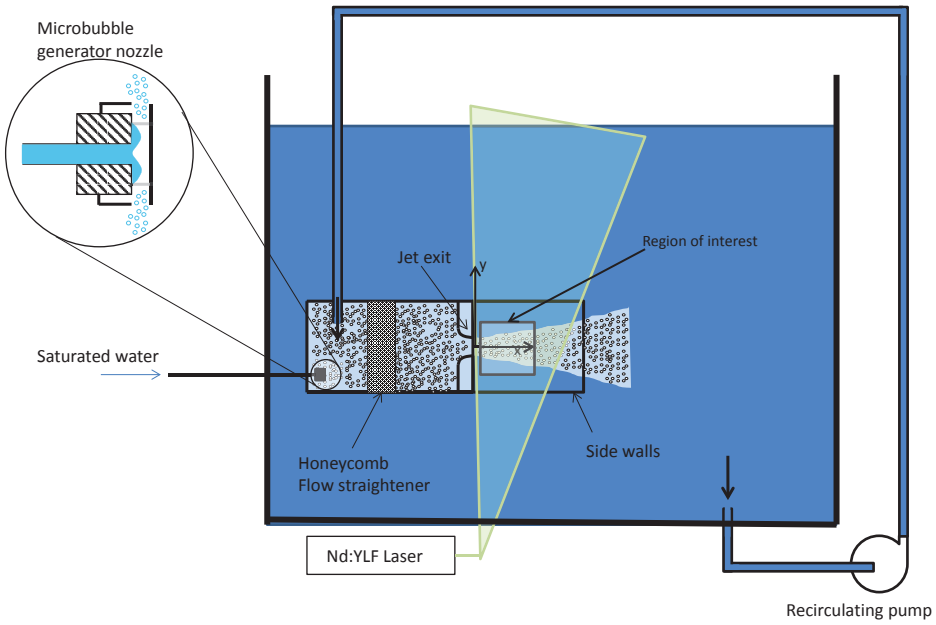

Figure 1. Schematic representation of the experimental setup and nozzle of the microbubble generation device

The plane jet consists of an upstream plenum (0.3 m × 0.2 m × 0.12 m, length×height×width) with a gauze homogenizer and a honeycomb flow straightener, and a jet nozzle manufactured with a 20 mm radial contraction of height $h = 4$ mm. The jet is confined by two parallel side walls $40h$ long, oriented in the $x-y$ plane to restrict jet spread in the lateral (z) direction. The microbubble generator was placed behind the honeycomb and below the flow inlet to promote the mixing of microbubbles before being advected through honeycomb and the jet nozzle. The plenum box was placed inside a large water tank with an outlet at the bottom to recirculate the flow.

Time-resolved PIV was used to record the velocity field from the jet exit to about $22h$ along centre of the jet in the $x-y$ plane. A double cavity Nd:YLF laser (Litron) with a maximum pulse energy of 2×22.5 mJ at 1 kHz (maximum repetition rate of 20 kHz) and output wavelength of 527 nm was used to generate the light sheet, and the edge aligned with the jet exit (see Figure 1). Images were acquired with a HighSpeedStar 8 CMOS 12-bit camera (LaVision) with a maximum resolution of 1024×1024 pixel and max frame rate of 7.5 kHz. Images were acquired at 2 kHz, allowing for mean bubble displacement of about 10 pixel in the region of interest. A total of 16001 images were acquired with a resolution of 83 μm/pixel. Images were interrogated with the commercial PIV software Davis 8.1 (LaVision). A multiple-pass spatial correlation algorithm between image pairs was used to resolve the velocity field. An initial 64×64 pixel interrogation subwindows with a 50% overlap was used, followed by decreasing interrogation subwindows sizes, down to 16×16 pixel with a 50% overlap for the final pass. The intermediate vector fields were post-processed with a median filter to remove outliers before decreasing the interrogation. The resulting vector field time-series was also post-processed with a median filter and a 3×3 pixel smoothing function. Details of the PIV algorithm can be consulted in [18, 14].

Results

Mean and Turbulent Flow Fields

Figure 2 shows the square of mean centreline streamwise velocity decay normalized by the jet exit centreline velocity ($U_{o,c}$), compared with the results from [10, 5, 4, 19]. It can be observed that the experimental results are within the range of measurement previously published. The dimensionless streamwise velocity profile U/U_c, where U_c is the local centreline velocity U_c, is presented in Figure 3. The downstream locations plotted show a self-similar behavior, in agreement with the Gaussian profile $f(y_n) = exp[-ln2(y_n)^2]$ [5], where $y_n = Y/y_{0.5}$ is the y-coordinate normalized by the velocity half-width ($y_{0.5}$).

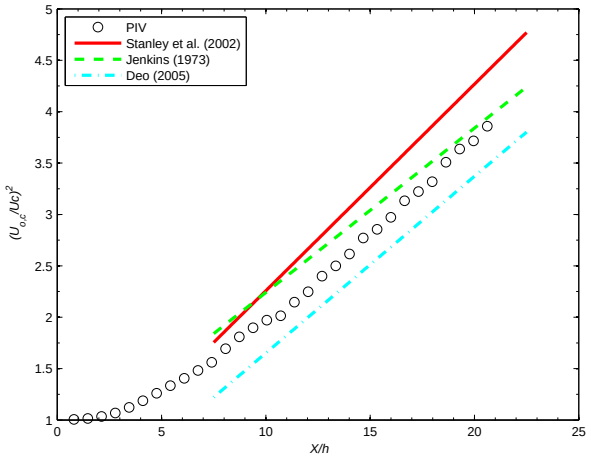

Figure 2. Decay of the streamwise centreline mean velocity compared previously published results

Figure 4 presents the streamwise and vertical root-mean-square (RMS) velocity profiles at three downstream locations. The RMS profiles are in good agreement with previously published results with similar Re [4, 16], and show the well konow change

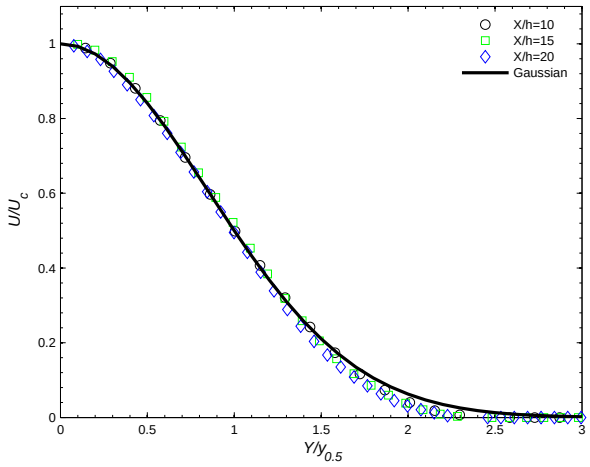

Figure 3. Dimensionless mean velocity profiles at three different streamwise location compared to the Gaussian profile $U_n = e^{-ln2(y_n^2)}$ from [5]

in turbulence intensity observed in the developing region of the plane jet.

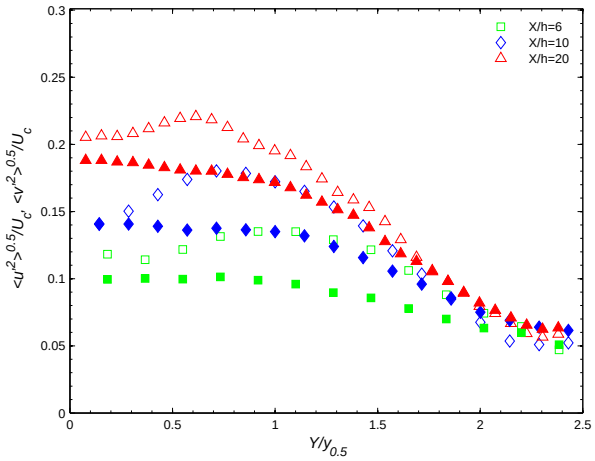

Figure 4. Dimensionless streamwise (open symbols) and vertical (closed symbols) velocity profiles at selected downstream locations

Coherent Structures

The coherent structures of the flow were resolved using proper orthogonal decomposition [11, 7] of the fluctuating velocity field. The method of snapshots [17] was used here. A total of 500 vector fields sampled at a reduced frequency of 100 Hz were used to ensure converged statistics and independent samples [15]. Figure 5 shows the percentage of the cumulative POD modes energy. About 50% of the energy is contained within the first 19 modes, of which 6.3% and 6% are contributed by the first and second modes, respectively. The first two modes and a reconstructed snapshot of the fluctuating velocity vector field for the region between $10h$ and $20h$ are presented in Figure 6. From the first two modes it can be observed that at about $10h$ to $15h$ there are three dominant coherent structures, two near the boundaries of the jet and one in the centre. Further downstream these merge into a single large coherent structure. A reconstruction of the fluctuating velocity field at a random time shows these structures moving downstream. These are in good

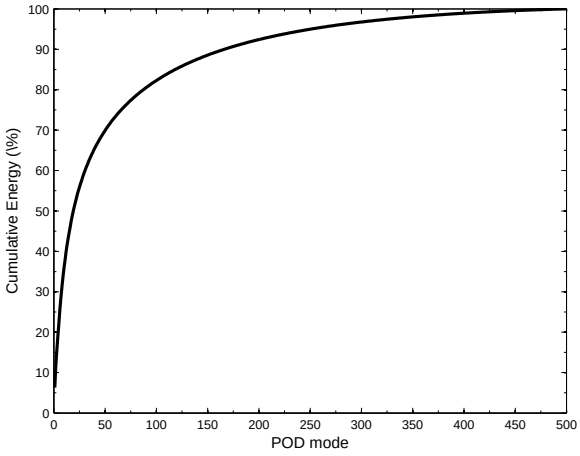

Figure 5. Cumulative energy contained in each POD mode.

agreement with the structures reported by [3, 16, 8].

Conclusions and Future Work

A microbubble generator using rapid expansion of supersaturated water through a confined radial jet was tested in a planar jet, a well characterized flow in the existing literature. The mean streamwise velocity decay, mean velocity profiles at several streamwise locations, and RMS streamwise and normal velocities were estimated and are in good agreement with previously published results. Proper orthogonal decomposition of the velocity fluctuation vectors was also carried out and showed that the dominant coherent structures are resolved and in agreement with previously published results. The results validate the use of microbubbles as seeding for PIV studies in turbulent flows. Further work is required describe the effects of nozzle geometry, flow rate, and pressure on the size distribution and production rate of the microbubbles. To further validate the use of microbubbles, it is recommended to conduct the same experiment using traditional solid seeding as a benchmark case.

Acknowledgements

This project was supported by the Defence Science and Technology Organisation (Mr. Brendon Anderson and Dr. David Clarke) and the University of Tasmania. The authors wish to thank Mr. Robert Wrigley and Mr. Steve Kent for their valuable help setting up the experiments.

References

[1] Brandner, P. A., Pearce, B. W., de Graaf, K. L., Zarruk, G. A. and Burgess, J., Microbubble generation in a confined radial jet, in *Proceedings of the 19th Australasian Fluid Mechanics Conference*, AFMS, Melbourne, Australia, 2014.

[2] Brandner, P. A., Wright, G., Pearce, B., Goldsworthy, L. and Walker, G. J., An experimental investigation of microbubble generation in a confined turbulent jet, in *Proceedings of the 17th Australasian Fluid Mechanics Conference*, AFMS, Auckland, New Zealand, 2010.

[3] Browne, L. W. B., Antonia, R. A. and Chambers, A. J., The interaction region of a turbulent plane jet, *Journal of Fluid Mechanics*, **149**, 1984, 355–373.

[4] Deo, R., *Experimental investigations of the influence of Reynolds number and boundary conditions on a plane air jet*, Ph.D. thesis, University of Adelaide, 2005.

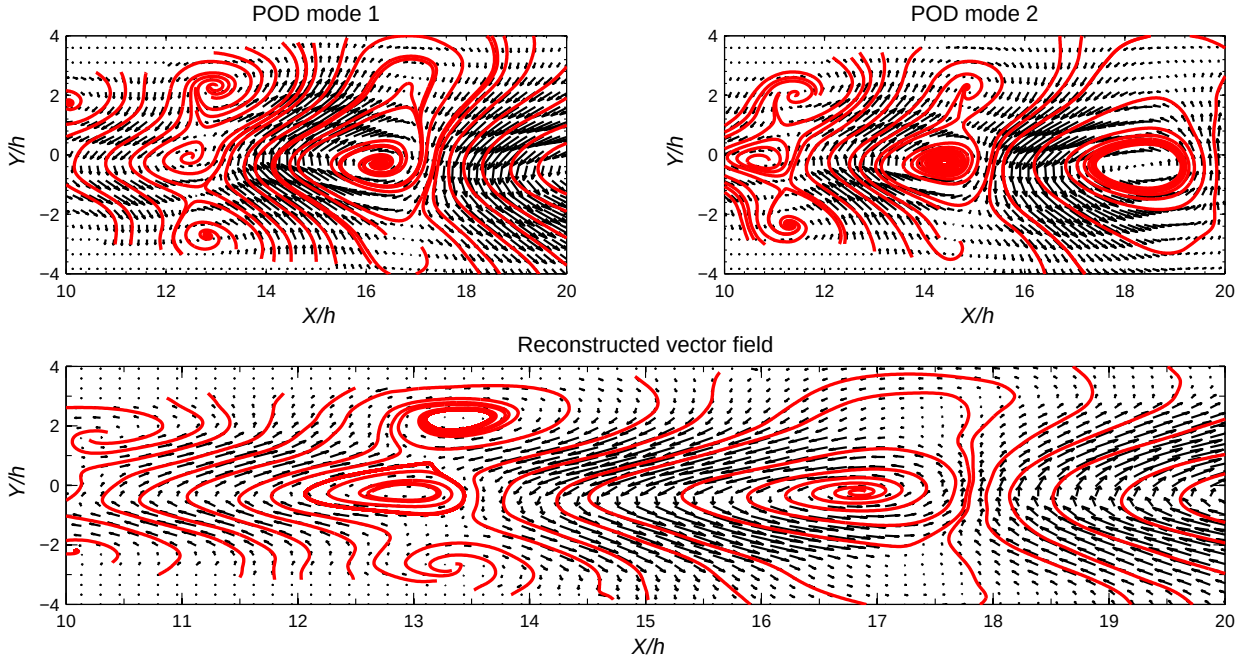

Figure 6. POD modes 1 (top-left) and 2 (top-right) represented by vectors and stream lines, and the velocity fluctuation vectors and streamlines (bottom) reconstructed from the first two POD.

[5] Deo, R. C., Mi, J. C. and Nathan, G. J., The influence of reynolds number on a plane jet, *Physics of Fluids*, **20**.

[6] Fujikawa, S., Zhang, R. S., Hayama, S. and Peng, G. Y., The control of micro-air-bubble generation by a rotational porous plate, *International Journal of Multiphase Flow*, **29**, 2003, 1221–1236.

[7] Gordeyev, S. V. and Thomas, F. O., Coherent structure in the turbulent planar jet. part 1. extraction of proper orthogonal decomposition eigenmodes and their self-similarity, *Journal of Fluid Mechanics*, **414**, 2000, 145–194.

[8] Gordeyev, S. V. and Thomas, F. O., Coherent structure in the turbulent planar jet. part 2. structural topology via pod eigenmode projection, *Journal of Fluid Mechanics*, **460**, 2002, 349–380.

[9] Hettiarachchi, K., Talu, E., Longo, M. L., Dayton, P. A. and Lee, A. P., On-chip generation of microbubbles as a practical technology for manufacturing contrast agents for ultrasonic imaging, *Lab on a Chip*, **7**, 2007, 463–468.

[10] Jenkins, P. E. and Goldschmidt, V. W., Mean temperature and velocity in a plane turbulent jet, *Journal of Fluids Engineering*, **95**, 1973, 581–584.

[11] Lumley, J. L., The structure of inhomogeneous turbulence, in *Atmospheric Turbulence and Wave Propagation*, editors A. M. Yaglam and V. I. Tatarsky, Doklady Akademii, Moscow: Nauka, 1967, 166–178.

[12] Rykaart, E. M. and Haarhoff, J., Behavior of air injection nozzles in dissolved air flotation, *Water Science and Technology*, **31**, 1995, 25–35.

[13] Ryu, Y., Chang, K.-A. and Lim, H.-J., Use of bubble image velocimetry for measurement of plunging wave impinging on structure and associated greenwater, *Measurement Science and Technology*, **16**, 2005, 1945.

[14] Scarano, F. and Riethmuller, M., Advances in iterative multigrid piv image processing, *EXPERIMENTS IN FLUIDS*, **29**, 2000, S51–S60, 3rd International Workshop on Particle Image Velocimetry, SANTA BARBARA, CALIFORNIA, SEP 16-18, 1999.

[15] Semeraro, O., Bellani, G. and Lundell, F., Analysis of time-resolved piv measurements of a confined turbulent jet using pod and koopman modes, *Experiments in Fluids*, **53**, 2012, 1203–1220.

[16] Shim, Y. M., Sharma, R. N. and Richards, P. J., Proper orthogonal decomposition analysis of the flow field in a plane jet, *Experimental Thermal and Fluid Science*, **51**, 2013, 37–55.

[17] Sirovich, L., Turbulence and the dynamics of coherent structures .1. coherent structures, *Quarterly of Applied Mathematics*, **45**, 1987, 561–571.

[18] Stanislas, M., Okamoto, K., Kahler, C. and Westerweel, J., Main results of the second international piv challenge, *Experiments in fluids*, **39**, 2005, 170–191.

[19] Stanley, S. A., Sarkar, S. and Mellado, J. P., A study of the flow-field evolution and mixing in a planar turbulent jet using direct numerical simulation, *Journal of Fluid Mechanics*, **450**, 2002, 377–407.

[20] van Overbruggen, T., Schroder, F., Klaas, M. and Schroder, W., A particle-image velocimetry tracer generating technique for liquid flows, *Measurement Science and Technology*, **25**, 2014, 087001 (4 pp.).